Effect of the Plasma Impedance on the Time Variation of the Inverse Pinch

AUTHOR(S):

WANI, Kisaburo; SAKURAI, Takeo

CITATION:

WANI, Kisaburo ...[et al]. Effect of the Plasma Impedance on the Time Variation of the Inverse Pinch. Memoirs of the Faculty of Engineering, Kyoto University 1969, 31(3): 332-344

ISSUE DATE:

1969-09-30

URL:

http://hdl.handle.net/2433/280782

Effect of the Plasma Impedance on the Time Variation of the Inverse Pinch

By

Kisaburo WANI* and Takeo SAKURAI*

(Received March 20, 1969)

The effect of the plasma impedance on the transient behavior of the inverse pinch is investigated. The initial value problem of the ordinary differential equation is formulated with respect to the electric current, the magnetic cavity radius, the shock front radius and the density behind the shock front within the frame work of reasonable assumptions. The present treatment is a refinement of the acoustic treatment by the senior author (T.S.) and affords qualitatively reasonable results even for cases where the acoustic treatment breaks down. The solution is obtained numerically by the standard method and the existense of a new type damped oscillation is clarified.

Section 1 Introduction

An electrically conducting circular cylinder is placed between parallel plates of perfect electric conductors with its axis of symmetry perpendicular to the plates and the space in between is filled up with the plasma (Fig. 1). The cylinder is connected to the electric power supply of timely constant electric potential by a cable free from the impedance after a certain instant of time. If the electric conductivity is infinite, the plasma is pushed outwards by the magnetic pressure

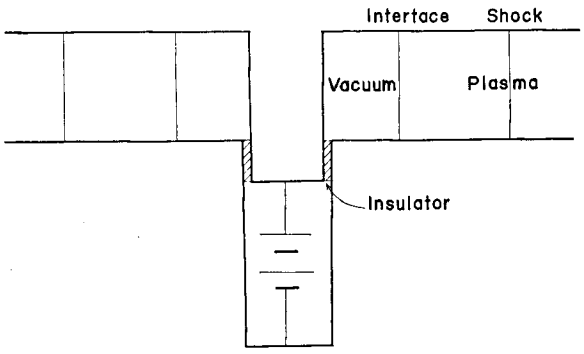

Fig. 1. Flow Configuration.

* Department of Aeronautical Engineering

and there appears a cavity region around the conducting cylinder because of the completely diamagnetic property of the infinitely conducting medium. The effect of this piston like motion of the vacuum-plasma interface is communicated into the plasma by the shock wave. On the other hand, the current through the cylinder is affected by the impedance of the system consisting of the circuit and of the plasma environment. All the changes continue until the equilibrium state is reached in which the magnetic pressure in the cavity region is balanced by the static pressure of the plasma.

This phenomenon is investigated by Sakurai within the frame work of the acoustic approximation and several interesting features are clarified[1] (Reference 1 is refered as Ref. 1 hereafter, and the reminders from the physical view point which are already mentioned in Ref. 1 is omitted as far as the self-containedness of the present paper is not violated.). His method, however, breaks down for cases with strong shocks where the initial speed of the vacuum-plasma interface exceeds that of the sound wave.

Because of its importance as a typical example of the plasma impedance and of the non-linear coupling system, this phenomenon is hoped to be explored in a more rigorous manner.

To achieve the first step refinement of the acoustic treatment within an endurable degree of the mathematical complexity, the following assumptions are made:

(1) The conducting circular cylinder is considered to have timely constant electric resistivity, and the inductance of the circuit other than that due to the plasma configuration to vanish.

(2) The plasma is considered to be continuum with the infinite electric conductivity and with the vanishing viscosity and the thermal conductivity.

(3) The displacement current is neglected in the Maxwell's equations and the energy density of the electric field is neglected in comparison to that of the magnetic field.

(4) The density behind the shock front is constant with respect to the space variables.

Assumptions (1) through (3) are the same as those in Ref. 1. Assumption (4) retains the character of the previous acoustic treatment in the form of the constancy of the density with respect to the space variables. The strength of the shock wave, on the other hand, is left free, and this freedom enables us to obtain results for every operating condition of the inverse pinch.

Section 2 The basic equations

Because of the geometrical symmetry, the flow of the plasma occurs radially in

the r-direction, the magnetic field azimuthally in the θ-direction and the electric field as well as the electric current axially in the z-direction, respectively, where the use is made of the cylindrical coordinates (r, θ, z) whose z axis coincides with the axis of the conducting cylinder. The inner plasma boundary and the shock front are concentric with z axis as the common axis of symmetry. The only space variable on which the physical quantities depend is r. Finally, MKS system of units is used throughout this paper.

By virtue of the assumption (3) and the fact that there is no electric current in vacuum, the magnetic field in the cavity region is obtained as follows:

$$B = \frac{\mu I}{2\pi r}, \tag{1}$$

where B, I and μ are the magnetic field, the total current through the conducting cylinder and the magnetic permeability, respectively.

By the usual procedure of the electromagnetic theory and the assumption (3), the following is obtained from Maxwell's equations:

$$\int_{\varepsilon}^{R}\left\{\frac{\partial}{\partial t}\left(\frac{\boldsymbol{B}^2}{2}\right)+\mathrm{div}(\boldsymbol{E}\times\boldsymbol{B})\right\}2\pi r dr = 0, \tag{2}$$

where $\boldsymbol{E}$, R and ε are the electric field, the cavity radius and the radius of the cylinder, respectively.

By virtue of the assumption (1), the energy afforded by the electric power supply is converted into heat by the Ohmic loss in the conducting cylinder and into the Poynting vector emanating from the surface of the cylinder. This leads to the following with respect to the unit length of z:

$$IV-\sigma I^2 = -\frac{2\pi\varepsilon}{\mu}(EB)_{r=\varepsilon}, \tag{3}$$

where DV, $D\sigma$ and D is the electric potential of the power supply, the resistance of the circular cylinder and the distance between the two parallel plates, respectively.

The substitution of Eqs. (1) and (2) into Eq. (3) leads to the following:

$$\frac{\mu}{2\pi}\frac{d}{dt}\left(I\log\frac{R}{\varepsilon}\right)+\sigma I = V. \tag{4}$$

By virtue of the assumptions (2) and (4) and the completely diamagnetic property of the infinitely conducting medium, the basic equations of the plasma flow behind the shock front are as follows:

$$\frac{d\rho}{dt}+\frac{\rho}{r}\frac{\partial(ru)}{\partial r} = 0, \tag{5}$$

$$\rho\frac{\partial u}{\partial t}+\rho u\frac{\partial u}{\partial r}=-\frac{\partial p}{\partial r}, \tag{6}$$

where u, ρ and p are the velocity, the density and the pressure, respectively.

The shock conditions on the shock front are as follows:

$$\rho_s(U-u_s)=\rho_0 U, \tag{7}$$

$$\rho_s(U-u_s)^2+p_s=\rho_0 U^2+p_0, \tag{8}$$

$$\frac{1}{2}(U-u_s)^2+\frac{\gamma}{\gamma-1}\frac{p_s}{\rho_s}=\frac{U^2}{2}+\frac{\gamma}{\gamma-1}\frac{p_0}{\rho_0}, \tag{9}$$

where U and γ are the velocity of the shock front and the ratio of the specific heats, and suffixes 0 and s refer to the states in front of and behind the shock front, respectively.

Integration of Eq. (5) leads to the following:

$$u=-\frac{r}{2\rho}\frac{d\rho}{dt}+\frac{1}{2\rho r}\frac{d(\rho R^2)}{dt}. \tag{10}$$

The solution of Eqs. (7) through (9) with respect to ρ_s, p_s and u_s leads to the following:

$$\frac{2}{\gamma+1}\left\{1-\frac{\gamma p_0}{\rho_0(ds/dt)^2}\right\}=1-\frac{\rho_0}{\rho}, \tag{11}$$

$$p_s=p_0+\frac{2\rho_0(ds/dt)^2}{\gamma+1}\left\{1-\frac{\gamma p_0}{\rho_0(ds/dt)^2}\right\}, \tag{12}$$

$$u_s=\frac{2(ds/dt)}{\gamma+1}\left\{1-\frac{\gamma p_0}{\rho_0(ds/dt)^2}\right\}, \tag{13}$$

where S is the shock front radius and use is made of the fact that ρ is constant with respect to the space variable: $\rho=\rho_s$. Elimination of u_s from Eqs. (10) and (13) leads to the following:

$$\frac{d}{dt}\left\{\rho(S^2-R^2)\right\}=\rho_0\frac{dS^2}{dt}. \tag{14}$$

Elimination of p_s from Eq. (6) (integrated with respect to r from R to S) and Eq. (12) leads to the following:

$$\begin{aligned}\frac{\mu I^2}{8\pi^2R^2}-p_0+\frac{\rho}{4}\frac{d}{dt}\left(\frac{1}{\rho}\frac{d\rho}{dt}\right)\cdot(S^2-R^2)-\frac{\rho}{2}\frac{d}{dt}\left\{\frac{1}{\rho}\frac{d(\rho R^2)}{dt}\right\}\cdot\log\frac{S}{R}\\ =\frac{\rho}{2}\left(\frac{dS}{dt}\right)^2\left\{1-\left(\frac{\rho_0}{\rho}\right)^2\right\}-\frac{\rho}{2}\left(\frac{dR}{dt}\right)^2.\end{aligned} \tag{15}$$

Eqs. (4), (11), (14) and (15) constitute the determined system of ordinary

differential equations with respect to I, R, S and ρ. This system of equations is non-dimensionalized as follows:

$$\xi\eta\frac{d}{d\tau}(i\log l)+\eta i=1\,, \tag{16}$$

$$\frac{2}{\gamma+1}\left\{1-\frac{4m}{(dm/d\tau)^2}\right\}=1-\frac{1}{d}\,, \tag{17}$$

$$\frac{d}{d\tau}\left\{d(m-l)\right\}=\frac{dm}{d\tau}\,, \tag{18}$$

$$\frac{1}{\gamma}\left(\frac{i^2}{l}-1\right)+\frac{d}{4}(m-l)\frac{d}{d\tau}\left(\frac{1}{d}\frac{dd}{d\tau}\right)-\frac{d}{4}\frac{d}{d\tau}\left\{\frac{1}{d}\frac{d(dl)}{d\tau}\right\}\log\frac{m}{l}$$
$$=\frac{d}{8m}\left(\frac{dm}{d\tau}\right)^2\left(1-\frac{1}{d^2}\right)-\frac{d}{8l}\left(\frac{dl}{d\tau}\right)^2\,, \tag{19}$$

where

$$l=\left(\frac{R}{\varepsilon}\right)^2,\quad m=\left(\frac{S}{\varepsilon}\right)^2,\quad d=\frac{\rho}{\rho_0},\quad i=\frac{I}{I_*},\quad \tau=t\Big/\frac{\varepsilon}{c_0}\,, \tag{20}$$

$$\xi=\frac{\mu c_0}{4\pi\varepsilon\sigma}=c_0\varepsilon\Sigma\mu,\quad \eta=\frac{I_*\sigma}{V},\quad I_*=\left(\frac{8\pi^2\varepsilon^2 p_0}{\mu}\right)^{1/2}\,, \tag{21}$$

and Σ and c_0 are the conductivity of the conducting cylinder and the velocity of sound, respectively.

Eqs. (16) through (19) are of the first order with respect to i, d, and m, and of the second order with respect to l. Similar to the situation in Ref. 1, the necessary initial conditions are obtained by the intuitively apparent conditions:

$$l_i=m_i=1\,,\qquad i_i,\ d_i\ \text{ and }\ \left(\frac{dl}{d\tau}\right)_i\ \text{ are all finite} \tag{22}$$

together with Eqs. (16) through (19):

$$\left(\frac{dl}{d\tau}\right)_i=\frac{1-\eta i_i}{\xi\eta i_i}\,, \tag{23}$$

$$d_i=\frac{4\xi^2\eta^2 i_i^2(i_i^2-1)}{4\xi^2\eta^2 i_i^2(i_i^2-1)-\gamma(1-\eta i_i)^2}\,, \tag{24}$$

$$\gamma(\gamma+1)(i_i^2-1)(1-\eta i_i)^2-8\xi^2\eta^2 i_i^2(i_i^2-1)^2+2\gamma^2(1-\eta i_i)^2=0\,, \tag{25}$$

where suffix i refers to the initial state.

Because of the fact that the initial value of $dl/d\tau$ is positive and non-zero only for the electric current larger than that which affords the magnetic pressure just enough to balance the undisturbed plasma pressure at the surface of the circular cylinder, i_i must be in the following range: $1/\eta>i_i>1$.

Substitution of $\gamma=5/3$ into Eq. (25) leads to the following:

$$f(i_i) = \frac{\sqrt{5}\,(1-\eta i_i)\sqrt{4i_i^2+1}}{6\xi\eta i_i(i_i^2-1)} - 1 = 0\,. \tag{26}$$

By the differentiation of $f(i_i)$ with respect to i_i, it is clarified that df/di_i is negative definite in the above range of i_i. This, together with the following: $\lim_{i_i\to(1/\eta)-0} f(i_i) = -1$ and $\lim_{i_i\to 1+0} f(i_i) = \infty$, leads to the unique existence of the real solution of Eq. (26) in the above range of i_i. Thus, our initial conditions assures the unique initiation of the evolution for given values of parameters.

Section 3 Semi-asymptotic behavior for moderately large values of τ

Since the shock front attenuates off, and the density and the pressure approach to those of the undisturbed state, the asymptotic state is described by the following expressions:

$$d = 1+d_1\,, \qquad d_1 \ll 1 \tag{27}$$

$$l = 1/\eta^2+l_1\,, \qquad l_1 \ll 1/\eta^2 \tag{28}$$

$$i = 1/\eta+i_1\,, \qquad i_1 \ll 1/\eta \tag{29}$$

$$m = \tau^2+m_1\,, \qquad m_1 \ll \tau^2 \tag{30}$$

where suffix 1 refers to the small deviation with respect to the first term. Substitution of the above into Eqs. (16) through (19) leads to the following:

$$d_1 = \frac{1}{\tau^2}\left(\frac{1}{\eta^2}-1\right), \tag{31}$$

$$m_1 = k\tau+\frac{k^2}{4}-\frac{\gamma+1}{2}\left\{\frac{1}{\eta^2}-1\right\}, \tag{32}$$

$$\xi\left\{\frac{di_1}{d\tau}\log\left(\frac{1}{\eta^2}\right)+\eta\frac{dl_1}{d\tau}\right\}+i_1 = 0\,, \tag{33}$$

$$-\frac{\log(\eta^2\tau^2)}{4}\frac{d^2l_1}{d\tau^2}+\frac{2\eta i_1-\eta^2 l_1}{\tau} = -\frac{1}{2\tau^2}\left(\frac{1}{\eta^2}-1\right), \tag{34}$$

where k in Eq. (32) is an arbitrary constant and only the most predominant terms are retained in the above formulae. Eqs. (33) through (34) coincide with those in Ref. 1 except the inhomogeneous term on the right hand side of Eq. (34). This corresponds to the present retainment of the small but non-vanishing pressure difference on the shock front.

Elimination of i_1 from Eqs. (33) and (34) leads to the following:

$$\log(\eta^2\tau^2)\left\{\xi\log\left(\frac{1}{\eta^2}\right)\cdot\frac{d^3l_1}{d\tau^3}+\frac{d^2l_1}{d\tau^2}\right\}$$
$$+\frac{4\eta^2}{\tau}\left[\xi\left\{\log\left(\frac{1}{\eta^2}\right)+2\right\}\frac{dl_1}{d\tau}+l_1\right]=2\left(\frac{1}{\eta^2}-1\right)\left\{\frac{1}{\tau^2}-\frac{2\xi}{\tau^3}\log\left(\frac{1}{\eta^2}\right)\right\}. \tag{35}$$

Restricting ourselves to the moderately large values of τ, the logarithmic terms of τ can be taken as constant because of its slow variation.

Thus, the solution is obtained as follows:

$$l_1=\sum_{n=1}^{3}l_{1n}e^{\lambda_n\tau}+(\text{special solution of inhomogeneous equation}), \tag{36}$$

where

$$a\lambda^3+b\lambda^2+c\lambda+d=0, \tag{37}$$

$$\left.\begin{aligned} a&=\xi\log(\eta^2\tau^2)\cdot\log\left(\frac{1}{\eta^2}\right),\\ b&=\log(\eta^2\tau^2),\\ c&=\frac{4\eta^2}{\tau}\xi\left\{2+\log\left(\frac{1}{\eta^2}\right)\right\},\\ d&=\frac{4\eta^2}{\tau}. \end{aligned}\right\} \tag{38}$$

As is shown in Eq. (28), η is the reciprocal of the ratio of the asymptotic radius of the cavity to the radius of the conducting cylinder. Thus, η is taken to be small in comparison to 1. This, in turn, leads to the smallness of c and d with respect to a and b in Eqs. (37) and (38). Taking into account this fact, Eq. (37) can be solved as follows:

$$\lambda_1=-\frac{b}{a}\left\{1-\frac{ac}{b^2}\left(1-\frac{ad}{bc}\right)\right\}, \tag{39}$$

$$\lambda_2=\frac{b}{3a}\left[-i\sqrt{3}\left\{\frac{a\sqrt{3bd}}{b^2}+\frac{3a}{2b}\left(\frac{c}{b}-\frac{ad}{b^2}\right)\right\}-\frac{3ac}{b^2}\left(1-\frac{ad}{bc}\right)e^{-(\pi/3)i}\right], \tag{40}$$

$$\lambda_3=\text{complex conjugate of }\lambda_2. \tag{41}$$

Substitution of Eq. (38) into Eq. (40) clarifies that the real parts of λ_2 as well as λ_3 are negative, and also that terms corresponding to these are predominant over that to λ_1 for small values of η. Thus, the semi-asymptotic behavior of the vacuum-plasma interface for the moderately large values of τ is the damped oscillation. The ratio of the absolute value of the imaginary to the real part of λ_2 (as well as of λ_3) being:

$$\left|\frac{I\lambda_2}{R\lambda_2}\right|\sim\left[\frac{\tau}{4\xi^2\eta^2}\log(\eta^2\tau^2)\right]^{1/2}, \tag{42}$$

the oscillating character reveals itself only when $\xi\eta$ is so small that the oscillation survives for several periods. As is shown numerically in the next section, the small ξ corresponds to the appreciable strength of the initial shock front. Thus, the appearance of the damped oscillation is the characteristic feature of the case with appreciably strong initial shock front. The occurence of this damped oscillation is due to the coupling of the restoring property of the plasma compressibility with the damping property of the electric current through the circuit without capacitance.

Substitution of Eq. (36) into the equations of the second order approximation shows that the second order approximation is certainly small with respect to the first order approximation within the frame work of the present treatment. The arbitrary constants in the above solution are k in Eq. (32), l_{1n}'s in Eq. (36) and the integration constant related to Eq. (33). Thus, we have enough freedom to match our semiasymptotic expression with the numerical solution of the initial value problem.

Our present approximation, on the other hand, certainly breaks down for very large value of τ. Since the period of the oscillation increases with τ proportionally to $\{\log(\eta^2\tau^2)\}^{1/2}$, however, our present expression is expected to continue smoothly with the asymptotic expression for truely large values of τ (see Ref. 1).

Section 4 Results and discussion

Numerical calculations are performed by the application of the Newton-Raphson's method on Eq. (26) and of the Runge-Kutta-Gill method of quadrature on Eq. (16) through (19) under the initial conditions (22) through (25). Calculations are executed for the combinations of parameters shown in Tab. 1 where the initial values of quantities are also shown. It is easily seen that the initial strength of the shock front becomes stronger as ξ decreases. Since ξ is the magnetic Reynolds number with respect to the cylinder radius, the sound velocity in the undisturbed plasma and the electrical conductivity of the cylinder, we arrive at an interesting paradox that the more difficult the electric current flows, the stronger becomes the initial strength of the shock front. Several evolutions of the cavity radius are shown in Figs. 2 through 7. The existence of the damped oscillations notified in the previous section is ascertained in Figs. 3 and 5. As is mentioned there, the damped oscillation does appear for the case with small values of $\xi\eta$. The corresponding evolutions of the density are shown in Figs. 8 through 10. Relatively wide validity of the acoustic treatment, except the very initial period of time is ascertained. Finally, the consistency of our assumption (4) is examined in Tab. 2 in which the constancy of the entropy along with the fluid particle on

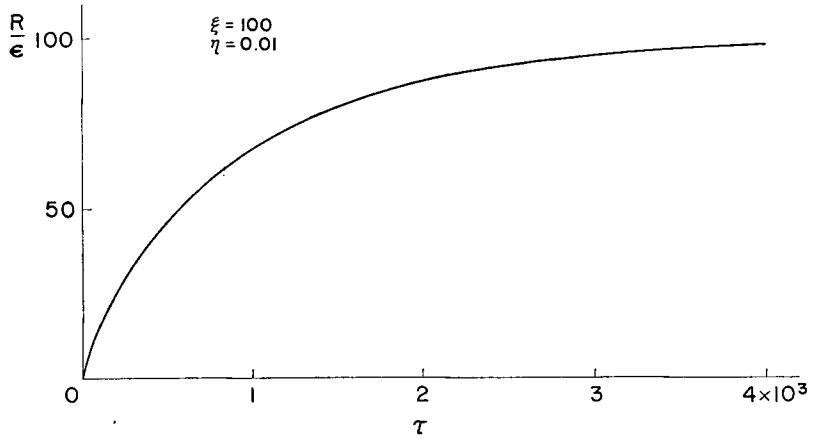

Fig. 2. Time Variation of R/ε.

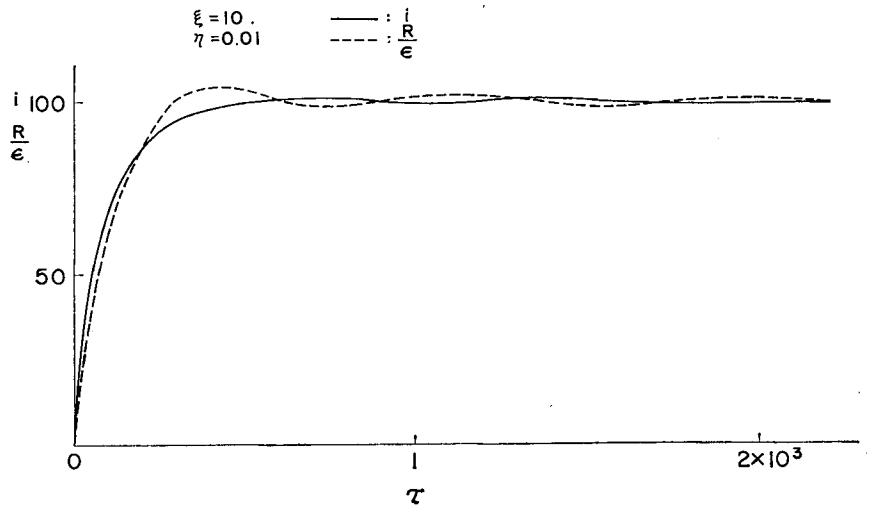

Fig. 3. Time Variation of R/ε and i

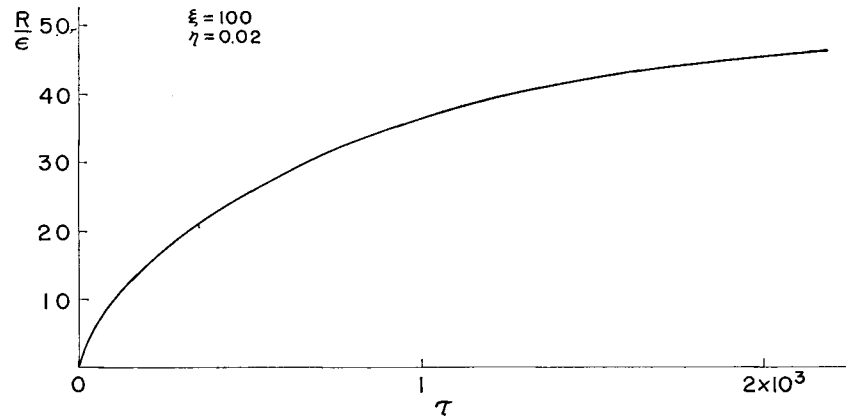

Fig. 4. Time Variation of R/ε.

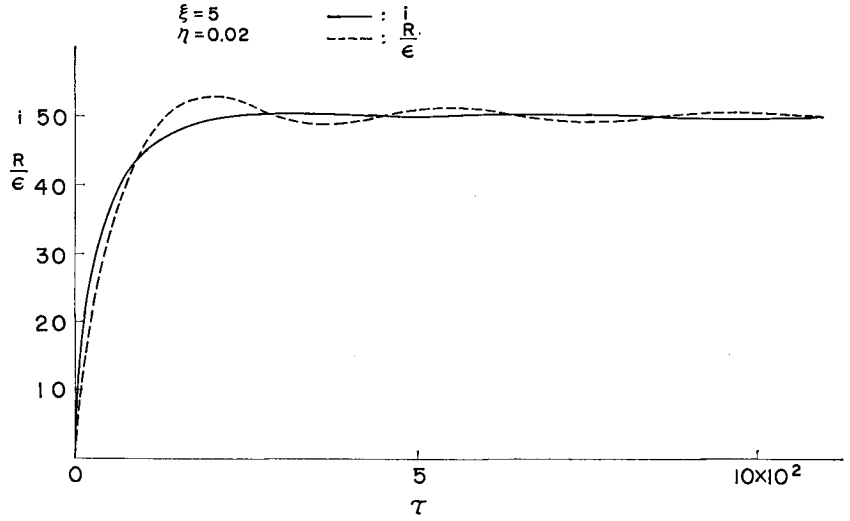

Fig. 5. Time Variation of R/ε and i.

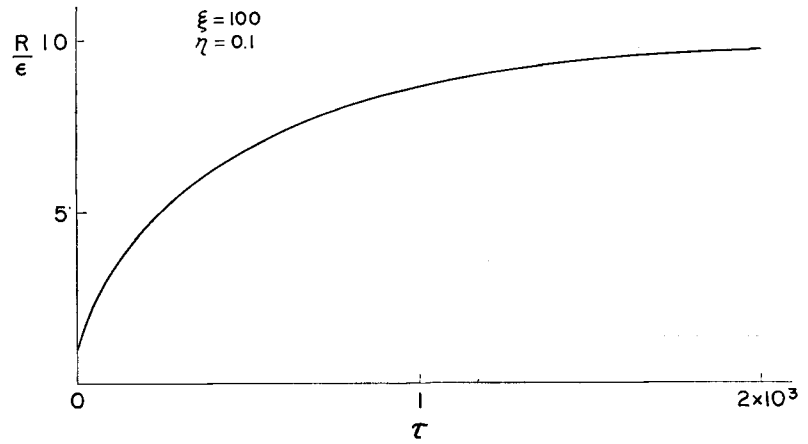

Flg. 6. Time Variation of R/ε.

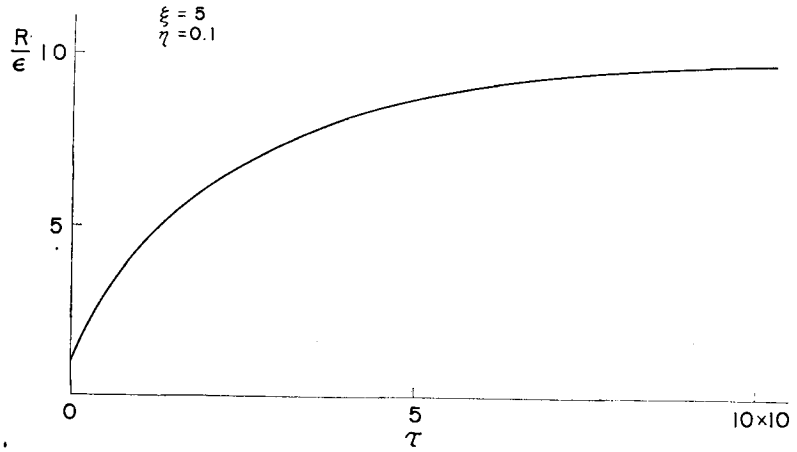

Fig. 7. Time Variation of R/ε.

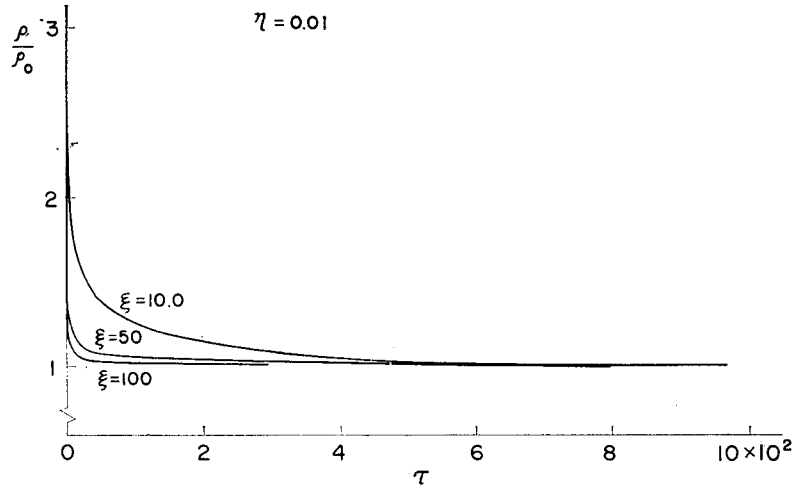

Fig. 8. Time Variation of ρ/ρ_0.

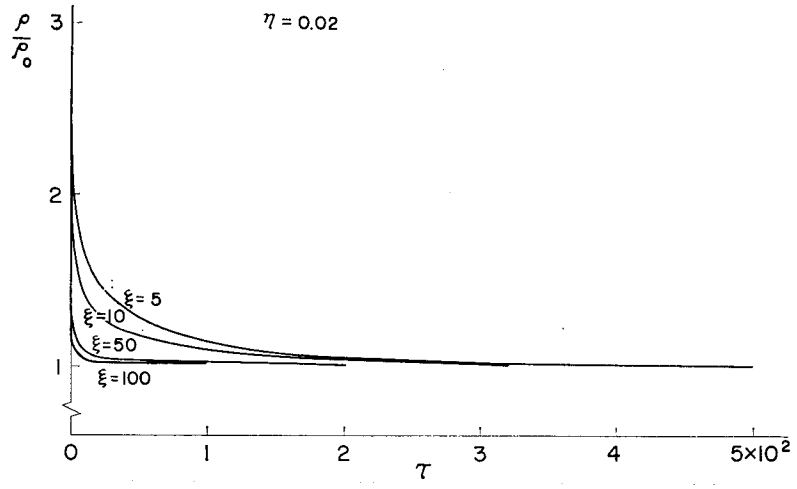

Fig. 9. Time Variation of ρ/ρ_0.

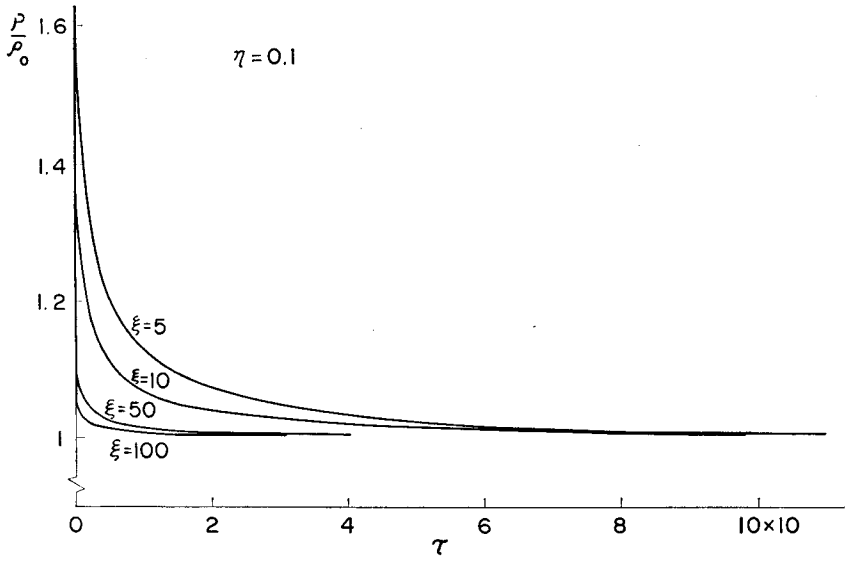

Fig. 10. Time Variation of ρ/ρ_0.

Table 1. values of quantities at $\tau=0$.

ξ	η	i	d	$\frac{di}{d\tau}$	$\frac{d}{d\tau}\left(\frac{R}{\varepsilon}\right)$	$\frac{d}{d\tau}\left(\frac{S}{\varepsilon}\right)$	$\frac{d}{d\tau}\left(\frac{\rho}{\rho_0}\right)$
100	0.2	1.0164	1.0197	0.0115	0.0196	1.0132	−0.0100
50	»	1.0323	1.0389	0.0228	0.0384	1.0260	−0.0200
10	»	1.1460	1.1770	0.1064	0.1681	1.1184	−0.0975
5	»	1.2644	1.3209	0.2002	0.2954	1.2162	−0.1884
100	0.1	1.0364	1.0439	0.0259	0.0432	1.0292	−0.0225
50	»	1.0709	1.0856	0.0511	0.0834	1.0571	−0.0448
10	»	1.3017	1.3659	0.2404	0.3341	1.2472	−0.2141
5	»	1.5262	1.6301	0.4572	0.5552	1.4365	−0.3972
100	0.02	1.1812	1.2197	0.1394	0.2067	1.1472	−0.1208
50	»	1.3323	1.4026	0.2752	0.3653	1.2728	−0.2349
10	»	2.1588	2.2680	1.3105	1.1081	1.9820	−0.8362
5	»	2.8523	2.7640	2.5441	1.6530	2.5901	−1.1269
100	0.01	1.3361	1.4072	0.2797	0.3692	1.2760	−0.2375
50	»	1.5930	1.7056	0.5517	0.6178	1.4933	−0.4400
10	»	2.8890	2.7850	2.6460	1.6808	2.6223	−1.1274
5	»	3.9290	3.2283	5.1782	2.4452	3.5425	−1.2416

Table 2. validity of our method.

ξ	η	α
100	0.2	0.997
50	0.2	0.993
10	0.2	0.962
5	0.2	0.929
100	0.1	0.992
50	0.1	0.984
10	0.1	0.938
5	0.1	0.886
100	0.02	0.966
50	0.02	0.947
100	0.01	0.937
50	0.01	0.914
$\alpha=\text{Max.}\{(p/\rho^\gamma)/(p/\rho^\gamma)_i\}$		

the vacuum-plasma interface is shown via the minimum value of $(p/\rho^\gamma)/(p/\rho^\gamma)_i$. The consistency for the case with not so strong initial shock is easily seen from this table. If the damped oscillation does occur, however, there appears the system of the secondary shock waves behind the main shock front as the consequence of the piling up of the compression waves. Our assumption certainly breaks down in such a situation, and more exact treatment is necessary to explore such cases.

Reference

1) T. Sakurai: J. Phys. Soc. Japan 25, (1968) 1671.